Extraction for Multilayer Ceramic Capacitor Vibration Induced Force

Yifan Ding¹, Jianmin Zhang², Mingfeng Xue³, Xin Hua⁴, Benjamin Leung⁵, Eric A. MacIntosh⁶, Chulsoon Hwang⁷

EMC Laboratory, Missouri University of Science and Technology, Rolla, MO-65401, USA

dingyif@mst.edu¹, hwangc@mst.edu⁷

Google Inc., USA

jianmin@google.com², mingfengx@google.com³, xihua@google.com⁴, benleung@google.com⁵, ericmac@google.com⁶

Abstract—Due to the piezoelectric characteristic of the MLCC dielectric BaTiO₃, the multilayer ceramic capacitor (MLCC) can vibrate when the supply voltage has AC components. The vibration of the MLCC will generate a force on the printed circuit board (PCB) it is connected to, causing the PCB to vibrate as well. The MLCC vibration-generated force is extracted using a measurement-simulation-based methodology in this paper. The force of an MLCC is first extracted at the PCB resonance frequencies. Then, a broadband force profile is obtained by using the interpolating method. The extraction methodology can be used in different boundary conditions, on different PCBs, and for different MLCCs with a good generalization.

Keywords—Multilayer ceramic capacitor (MLCC), piezoelectric characteristic, vibration velocity, force, laser doppler vibrometer (LDV)

I. INTRODUCTION

Nowadays electronic devices are following the trend of being compact and lightweight, which also brings the demand for compact electronic components higher and higher. Multilayer ceramic capacitor (MLCC) is in general a good choice in the printed circuit board (PCB) design for reducing the power distribution network (PDN) impedance to ensure low voltage ripple and maintain the system stability. It is also widely used because of the thin dielectric layers with the high permittivity dielectric of BaTiO₃. However, the dielectric of BaTiO₃ has the piezoelectric characteristic. After the MLCC is mounted on the PCB, with the application of an alternating electric field, it will expand and contract following the change of the electric field. And the effect of expanding and contracting movement acts like a force applied to the board as shown in Fig. 1. As a result, the board with MLCCs mounted will vibrate following the same frequency as the power rail noise. If the voltage noise has frequency components in the audible range from 20 Hz to 20 kHz, it is very likely to result in audio noise from PCB. This noise is usually regarded as the "singing cap" induced eNoise. It seems to be a very small noise, however, when happening in electronic devices such as earbuds, it quickly becomes noticeable thus degrading the user's listening experience. Moreover, the energy transfer from the electrical form to mechanical form causes the power dispassion and thus may degrade the PDN performance.

Research and study of the MLCC vibration can be found in recent literature. Simulation and measurement methodologies for the MLCC-induced acoustic noise are investigated in [1] and [2]. A practical and automatic simulation methodology for MLCC-based acoustic noise analysis is provided in [3]. Some methods addressing the eNoise reduction are discussed and given in [4] – [8].

However, this work mainly focuses on the specific outcome of the MLCC vibration – the acoustic noise, but hardly on the equivalent force excitation itself. As stated before, a very important intermediate product of MLCC

vibration is the force it applies to the PCB. Some work has been done about the force. In [9], the development and normalization of a novel sensor system built with low-cost industrial-grade multilayer ceramic capacitors (MLCC) is given, and in [10] the sensor is applied in a real product, which gives a good reference that the MLCC vibration induced force is measurable and quantifiable. However, the method proposed therein relies on an additional built-in circuit which requires more space on the compact PCB and thus is not convenient. A more straightforward and efficient way is required to extract and quantify the force induced by the MLCC vibration.

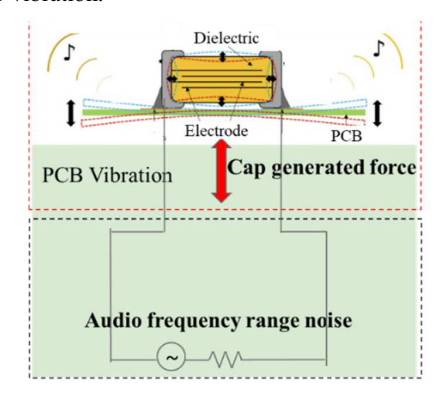


Fig. 1. PDN power rail noise caused electrical component vibration

It is always preferred that the measurement system has negligible impact if there is any on the device under test (DUT). Considering the use case of the MLCC, the PCB platform can be regarded as the medium to extract the MLCC vibration force. The vibration can be measured using the instrument laser doppler vibrometer (LDV). Also, the PCB design can be also obtained and input to the simulation. If the external loaded force to the PCB in the measurement or simulation has the same resultant vibration pattern and amplitude, then the unknown equivalent force from the MLCC can be derived. The above idea has been implemented and validated in [11]. The same methodology will be employed here to extract the force of MLCCs.

This paper is organized as follows: Section II will briefly summarize the MLCC force extraction flow with an application example. The results analysis for the measurement, simulation, and extension of the extracted MLCC vibration-generated force will be given in Section III. Section IV concludes the achievements in this paper and gives the future directions of this work.

II. MLCC FORCE EXTRACTION FLOW AND SETUP

The MLCC force extraction flow proposed and detailed in [11] is shown in Fig. 2. The method utilizes the PCB vibration velocities at the resonances with an external force added to the PCB system in the measurement and also in the corresponding

simulation model. The details will be introduced along with the application example in the following sections.

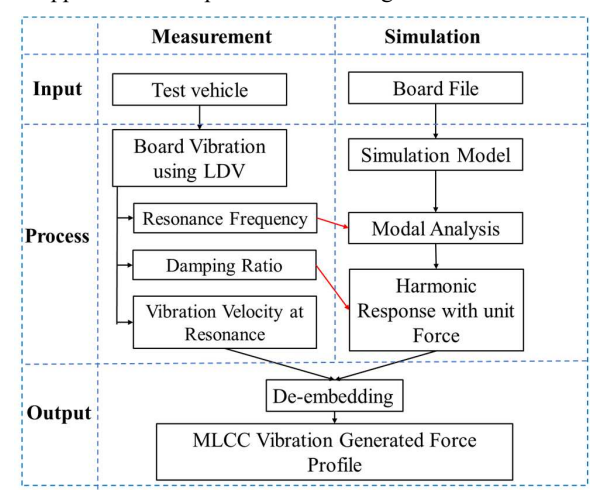


Fig. 2. MLCC vibration caused force extraction flow [11]

The general equation of motion [12] given in (1) provides the basic theoretical support for the force extraction flow, where the matrices can be obtained from the design file, and the vectors can be measured and simulated.

$$[M]\{\dot{u}\} + [C]\{\dot{u}\} + [K]\{u\} = \{F(t)\}$$
(1)

where [M] is the structural mass matrix, [C] is the structural damping matrix, [K] is the structural stiffness matrix, [F] is the load vector, $\{\ddot{u}\}$ is the nodal acceleration vector, $\{\dot{u}\}$ is the nodal velocity vector, $\{u\}$ is the nodal displacement vector, and (t) is the time.

A. Measurement

The input of the measurement process is the medium PCB with the target MLCC soldered on it. Power noise within the audio frequency range is applied to the power rail. The PCB used as a medium to extract the force generated by the MLCC is shown in Fig. 3. This is a 4-layer PCB with a dimension of 39.56 mm * 56.56 mm. There are 9 locations designed for capacitor soldering. The capacitor under test is the Murata 0603 in 22 uF. It is soldered on the pad near the middle of the short side of the PCB where for all the modes it would not be at the location with small resonance. The 1V DC nominal supply voltage with a 0.4Vpp AC noise in different frequencies is the input to the capacitor.

The LDV system is used to detect the DUT vibration. The measurement setup for the MLCC vibration-generated force extraction is shown in Fig. 4 and Fig. 5. The DUT, which is introduced before as the input of the measurement process is placed on the isolation table and within the range of the laser from the laser head. The control system controls the laser scanning and it can also generate the input signal to the DUT using the built-in signal generator. The input signal from the LDV control system is connected to the PCB input port using an external wire. Then the electrical signal reaches the MLCC through the traces of the PCB. The impact of the traces and the external wire to the PCB vibration is much smaller than the PCB vibration caused by the MLCC. The external wire is very light weight and very loose when connected with the PCB. No stretch force was added to the PCB. The PCB self-vibration without the capacitor excitation is also checked. The MLCC caused PCB vibration on the focused resonance mode is much beyond the noise floor.

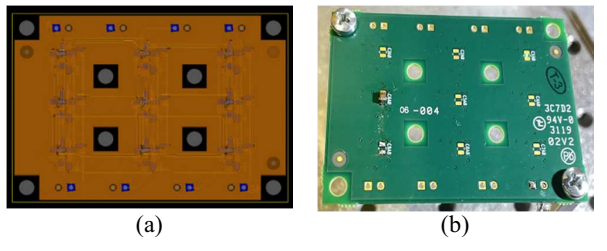


Fig. 3. PCB used for the force extraction. (a).design view (b) real PCB

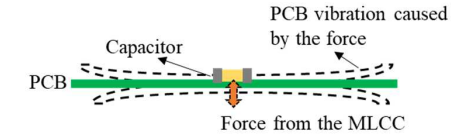


Fig. 4. Side view of the PCB with MLCC

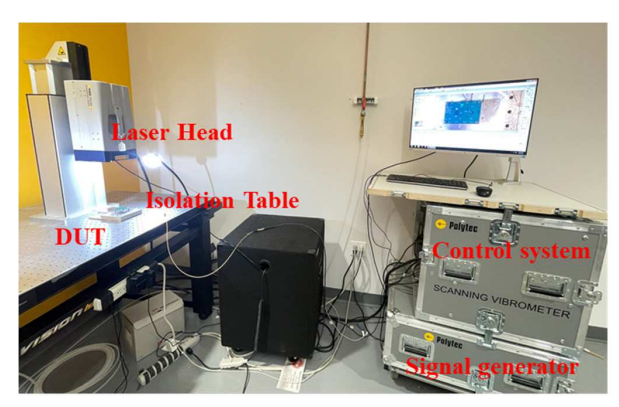


Fig. 5. Overview of the measurement setup

Three quantities are obtained when the board is vibrating: the PCB resonance frequencies, the damping ratios, and the PCB vibration velocities at the resonances. The resonance frequencies are the criterion to ensure the simulation model has good accuracy for the representation of the experimental DUT. Most importantly, the vibration velocities at the PCB resonances are measured and recorded. The velocities at the resonances are chosen on purpose for the large vibration amplitude and thus high measurement accuracy. The damping ratios are calculated from the measured PCB responses using the half-power method [13]. They are essential for mimicking the system's oscillating behavior and will be applied in the simulation. The damping ratios are obtained by applying equation (2) to the measured PCB vibration velocity response curves.

$$\gamma = \frac{\Delta\omega}{2\omega} \tag{2}$$

where $\Delta\omega$ is the normalized bandwidth of the resonant response at the amplitude of 0.707 v_{max} , and ω_r is the resonance frequency.

Due to the PCB size limitation, there are only a few resonances can be captured in the measurement frequency range for a given boundary condition configuration. Fortunately, the mode resonance frequencies will move as boundary conditions are changed. Thus, measurements are repeated with a few different boundary conditions to collect data at more discrete frequencies.

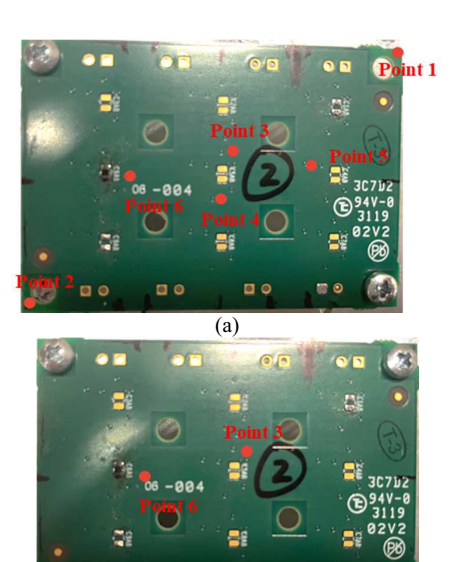


Fig. 6. Overview of the PCB with different boundary conditions with the observation points for PCB vibration velocity measurement (a) 2-fixed points (two screws at the top-left and right-bottom corner) (b) 4-fixed points (four screws at the four corners)

The overview of the PCB with different boundary conditions is shown in Fig. 6. For different boundary conditions, different observation points are selected based on the mode pattern and response. In order to obtain a sufficiently high measurement accuracy, the vibration velocity of the observation points should be relatively large for all the focused modes, so that the influence of the noise floor on the measurement results can be reduced. By comparing the all the resonance patterns on the focused modes, the observation points for the two boundary conditions are chosen as shown in Fig. 6. For all the modes, the vibration is measurable and accurate enough for the force extraction.

After the measurement, for each mode response, the results from different locations will be taken as the average to reduce the run-to-run variation. The PCB with two-screw and four-screw fixed points is used in the application example.

B. Simulation

The input of the simulation is the board file for the test PCB in the measurement process. The simulation is done in Ansys Mechanical. The stack-up information such as the layer thickness and equivalent material properties is assigned based on the design parameters. Boundary conditions are defined the same as the measurement. Taking the 2-fixed points boundary conditions as an example, at the spot where the PCB is fixed using the screw, a ring-shaped contact interface is modeled in the simulation. As shown in Fig. 7, the circles with the same radius and locations as the screws are defined as the boundary condition in the simulation. At last, the mesh density setting check is required to guarantee a converged result.

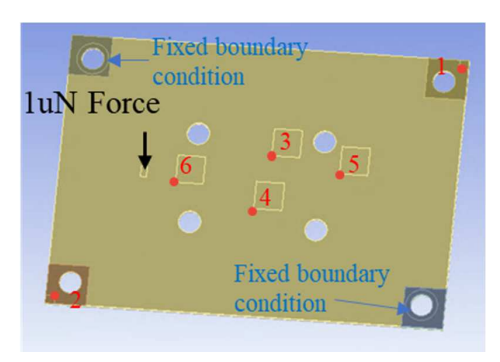


Fig. 7. Simulation model for 2-fixed points boundary condition

TABLE I. PCB SELF-RESONANCE FREQUENCY (Hz) COMPARISON FOR 2-FIXED POINTS BOUNDARY CONDITION

Mode	Measurement	Simulation	Δ
1	390.25	417.93	7.09%
2	1212	1173	3.22%
3	1558.125	1590.1	2.05%
4	2147.5	2095.5	2.42%
5	2817	2674.3	5.07%

TABLE II. PCB SELF-RESONANCE FREQUENCY (Hz) COMPARISON FOR 4-FIXED POINTS BOUNDARY CONDITION

Mode	Measurement	Simulation	Δ
1	967.5	982.21	1.52%
2	2296.25	2388.6	4.02%
3	2452.5	2530.7	3.19%

The modal analysis is first performed after the above settings are done properly. The results of the modal analysis are the system resonance frequencies. Comparing the resonance frequencies for different modes and different boundary conditions, the accuracy of the simulation model can be verified. For the application example used in this paper, the measurement and simulation model have a good correlation in terms of resonance frequencies as shown in TABLE. I and TABLE. II.

Then, the harmonic response analysis is followed. The result of this step is the PCB vibration velocity frequency response. Before that, the damping ratio extracted from the measured response is applied to the simulation setup. Also, the observation points are imprinted in the simulation model in the same locations as the measurement. The unifying force of luN is finally applied to the same location where the MLCC is mounted on the PCB. The velocities for different frequencies and different locations can be obtained.

C. Force Extraction

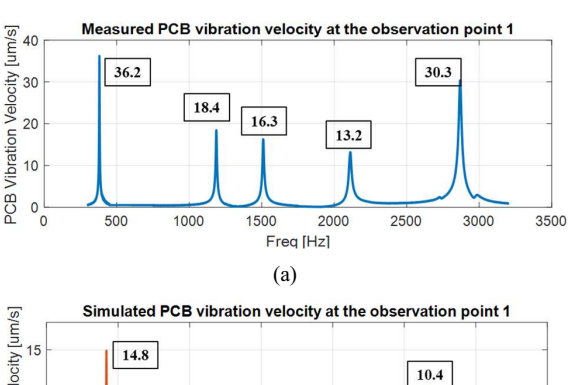
So far, two kinds of PCB vibration velocities have been obtained after the above measurement-simulation process. One is from the measurement caused by the MLCC vibration. The other is from the simulation with a unit force. The force from the MLCC is extracted by doing the de-embedding process, which refers to taking the ratio of the above two mentioned velocities. The reasons for doing so are given in [11] and are summarized as below.

1) If the different forces loading to the PCB from different sources at the same locations are with the same amplitude and injection angle, the impacts to the PCB vibration are the same. 2) The PCB vibration velocity change is proportional to the applied force change because the PCB mechanical system is linear with a small force excitation.

III. RESULTS ANALYSIS

The measurement and simulation results obtained in the force extraction process, as well as the analysis and discussions, will be given in this section.

The measured PCB frequency responses with the MLCC vibrating are checked first. For example, for the case with 2 fixed points, the measured velocity response at the observation point 1 for different frequencies is shown in Fig. 8 (a) and the PCB vibration velocities at different modes are marked. As stated in Section II. C, the velocities at the mode resonance frequencies are used to do velocity de-embedding to extract the MLCC force. Following the same procedure, the velocity response at different locations under different boundary conditions are recorded for further analysis.



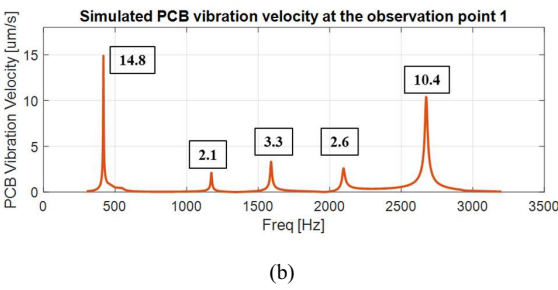


Fig. 8. Velocity response at observation point 1 for the case with 2-fixed boundary condition. (a) Measured response with MLCC force (b) Simulated response with the unit force.

Next step is to extract the damping ratios based on equation (2). Fig. 9 shows the averaged damping ratios from all the observation points, at each discrete mode resonance frequency, for the case with 2 fixed points. For this specific test vehicle, the damping ratio within the frequency range from around 400 Hz to 3000 Hz is pretty constant, which is about 0.35%.

The damping ratios are used as an input setting of the harmonic response simulation in Ansys Mechanical to correctly mimic the damping behavior of the system. Other settings as indicated in Section II are also done properly. Then, the PCB frequency responses with the unit force applied at the MLCC mounting location are simulated. For the case with 2 fixed points, the simulated velocity responses at observation point 1 for different frequencies are shown in Fig. 8 (b). Similarly, the PCB vibration velocities at different modes are noted and recorded for the force extraction.

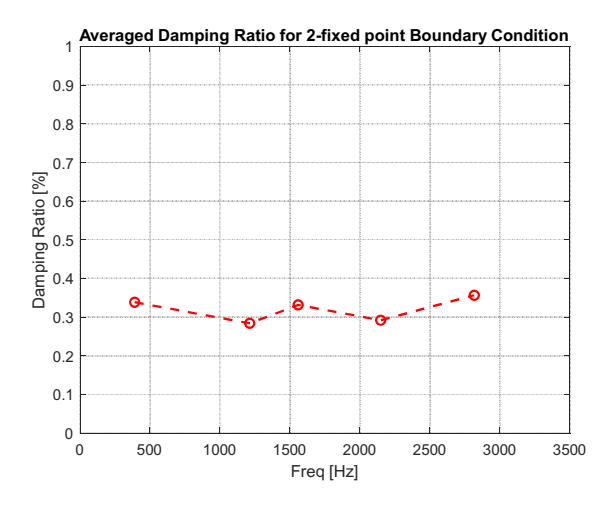


Fig. 9. Averaged damping ratio from all the observation points for 2-fixed point boundary conditions

The resonance frequencies in Fig. 8 are corresponding to the frequencies listed in TABLE I. The discrepancy between the measured and simulated resonance frequencies are reasonable. The simulation model is built based on the PCB geometry and the material property of the design file. There may be some differences between the parameters of the actual PCB and the designed one due to the manufacturing process. Also, when simulating for the mode resonance frequencies the fixed boundary conditions are added using the ideal fixation, while in the measurement the boundary condition is using the screws to fix. However, even if there are small discrepancies between the frequencies from measurement and simulation, the behavior of the PCB vibration should be the same, and it is reasonable to regard the resonance frequencies from the measurement and simulation aligned and do the velocity deembedding for the velocity at those frequencies.

The next step is the velocity de-embedding for the MLCC force extraction. The numbers noted in Fig.8 (a) and (b) are the PCB vibration velocities from measurement with MLCC force and from simulation with the unit force at the focused modes. By taking the ratio of the measured velocity and the simulated velocity at the corresponding mode resonance frequencies, the force loaded to the PCB can be extracted from this observation point. After de-embedding the velocities for all the resonances and taking the average of the forces extracted from the selected observation points, the extracted forces in the case with 2-fixed points boundary condition and 4-fixed points condition for different frequencies are shown in Fig. 10 in red circles and blue circles, respectively. For the focused mode frequencies, all the forces from the selected observation points have a convergence trend. It shows the consistency of measurement results.

Plotting the extracted forces of the case with 2 and 4-fixed points conditions, it shows that all these forces are within a relatively small range. The curve fitting method is implemented to get the force profile for the whole frequency range of interest. In the fitting process, the polynomial fitting method of different orders is used to predict the unknown MLCC vibration-induced force pattern. Fig. 10, shows the predicted force profiles when the order of the polynomial changes from 0 to 3. Other fitting methods can be used as well and the prediction results may differ.

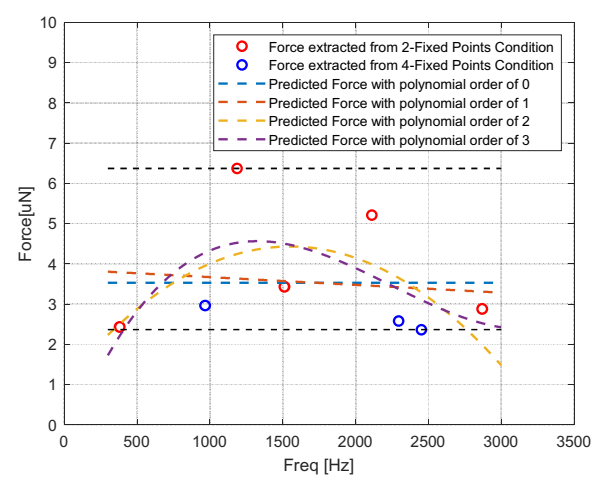


Fig. 10. MLCC force profile prediction using different polynomial orders for fitting

It can be observed that the level of the MLCC vibration generated force is around several micron-Newton when the MLCC is under the nominal supply voltage. Moreover, the deviation range among the forces extracted from different boundary conditions is relatively small, which verifies that the force generated by the MLCC vibration is independent of the boundary conditions. Therefore, more boundary conditions can be used to provide more force data at different resonance frequencies to improve the force prediction accuracy.

IV. CONCLUSIONS

In this paper, the force induced by the on-PCB MLCC vibration is extracted. The force when the MLCC is the under nominal condition is in the micron-Newton level. The extracted forces are for specific frequency points first and then extended to a broadband force profile using the polynomial fitting method.

In the current work, the frequency range covered is from 400 Hz to 3000 Hz. Other portions of the audible frequency band (20Hz - 20kHz) are not included due to the size limitation of the PCB under test. Future work can utilize PCBs of smaller or larger sizes to collect data in higher or lower frequencies within the audible frequency range using the same force extraction method.

As an interesting extension, the extracted and predicted force profile can be further validated by applying the force on different board configurations or applying the force at different locations of the same board and then comparing the predicted board vibration response with the real measured board vibration response.

Additionally, a transfer function between the electrical input (supply voltage level) and mechanical output (MLCC vibration generated force) can be derived by sweeping the voltage applied to the MLCC. A library can be further built for different types of MLCCs. This voltage-force relationship from the library can play as the input of the MLCC-induced eNoise modeling and prediction at the system level.

Through a more comprehensive study on the vibration force of MLCC, it is possible to better optimize the MLCC on the PDN, thereby reducing the impact of MLCC vibration on the electronic system.

REFERENCES

- [1] Y. Sun, S. Wu, J. Zhang, C. Hwang and Z. Yang, "Simulation Methodologies for Acoustic Noise Induced by Multilayer Ceramic Capacitors of Power Distribution Network in Mobile Systems," in *IEEE Transactions on Electromagnetic Compatibility*, vol. 63, no. 2, pp. 589-597, April 2021, doi: 10.1109/TEMC.2020.3019438.
- [2] Y. Sun, S. Wu, J. Zhang, C. Hwang and Z. Yang, "Measurement Methodologies for Acoustic Noise Induced by Multilayer Ceramic Capacitors of Power Distribution Network in Mobile Systems," in *IEEE Transactions on Electromagnetic Compatibility*, vol. 62, no. 4, pp. 1515-1523, Aug. 2020.
- [3] X. Yan, S. Wu, M. Xue, C. K. B. Leung, D. Beetner and J. Zhang, "A Practical Simulation Methodology for Singing Capacitor Based Acoustic Noise Analysis," 2022 IEEE International Symposium on Electromagnetic Compatibility & Signal/Power Integrity (EMCSI), 2022, pp. 29-33.
- [4] D. Kim, B.-H. Ko, S. Jeong, N.-C. Park and Y.-P. Park, "Vibration reduction of MLCC considering piezoelectric and electrostriction effect," 2015 Joint IEEE International Symposium on the Applications of Ferroelectric (ISAF), International Symposium on Integrated Functionalities (ISIF), and Piezoelectric Force Microscopy Workshop (PFM), 2015, pp. 186-189.
- [5] C. Covaci, F. Burza and T. Krausz, "MLCC Acoustic Noise Mitigation via Appropriate Design," 2022 IEEE 9th Electronics System-Integration Technology Conference (ESTC), 2022, pp. 488-491.
- [6] B. -H. Ko, D. Kim, N. -C. Park and Y. -P. Park, "Study on effective piezoelectric coefficient for finite element analysis of multi-layer ceramic capacitor," 2015 Joint IEEE International Symposium on the Applications of Ferroelectric (ISAF), International Symposium on Integrated Functionalities (ISIF), and Piezoelectric Force Microscopy Workshop (PFM), 2015, pp. 64-66.
- [7] H. Baek, D. Yu, J. Lee, H. Shim and J. -H. Kim, "Electrical approach to acoustic noise for MLCCs of power delivery network in mobile system," 2015 IEEE Electrical Design of Advanced Packaging and Systems Symposium (EDAPS), 2015, pp. 62-66.
- [8] S. Levikari, T. J. Kärkkäinen, P. Silventoinen, C. Andersson and J. Tamminen, "Acoustic detection of cracks and delamination in Multilayer Ceramic Capacitors," 2017 IEEE 11th International Symposium on Diagnostics for Electrical Machines, Power Electronics and Drives (SDEMPED), 2017, pp. 622-627.
- [9] K. -R. Lin, C. -H. Chiang, C. -H. Chang and C. -H. Lin, "Development of a novel force sensor system built with an industrial multilayer ceramic capacitor (MLCC)," 2012 7th IEEE International Conference on Nano/Micro Engineered and Molecular Systems (NEMS), 2012, pp. 487-490.
- [10] K. -R. Lin, T. -H. Liu, S. -W. Lin, C. -H. Chang and C. -H. Lin, "Occlusive bite force measurement utilizing flexible force sensor array fabricated with low-cost multilayer ceramic capacitors (MLCC)," TRANSDUCERS 2009 - 2009 International Solid-State Sensors, Actuators and Microsystems Conference, 2009, pp. 2238-2241.
- [11] Y. Ding, J. Zhang, M. Xue, X. Hua, B. Leung, E. A. MacIntosh, and C. Hwang, "Equivalent Force Extraction Methodology for Electrical Component Vibration on PCB", in *IEEE Transactions on Electromagnetic Compatibility*, submitted.
- [12] A. A. Shabana, Theory of vibration. New York: Springer-Verlag, 1991.
- [13] U. Zaheer and M. Ajmal, "Comparison of Damping Estimation Techniques for Flight Tests," 2019 16th International Bhurban Conference on Applied Sciences and Technology (IBCAST), 2019, pp. 243-247.